Characterization of Null Mutants of the Glyoxylate Cycle and Gluconeogenic Enzymes in *S. cerevisiae* Through Metabolic Network Modeling Verified by Chemostat Cultivation

I. Stückrath,[1*] H. C. Lange,[2] P. Kötter,[1] W. M. van Gulik,[2] K.-D. Entian,[1*] J. J. Heijnen[2]

[1]Institut für Mikrobiologie, J.W. Goethe-Universität Frankfurt, Germany
[2]Kluyver Laboratory for Biotechnology, Technical University Delft, The Netherlands, telephone: +31(15)278-2998; fax: +31(15)278-2355; e-mail: h.c.lange@tnw.tudelft.nl

Received 18 April 2001; accepted 10 September 2001

Abstract: Biomass yields for several null mutants in *Saccharomyces cerevisiae* were successfully predicted with a metabolic network model. Energetic parameters of the model were obtained from growth data in C-limited aerobic chemostat cultures of the corresponding wild-type strain, which exhibited a *P/O* ratio of 1.46, a non-growth-related maintenance of 56 mmol ATP/C-mol biomass/h, and a growth-related requirement of 655 mmol ATP/C-mol biomass. Biomass yields and carbon uptake rates were modeled for different mutants incapacitated in their glyoxylate cycle and their gluconeogenesis. Biomass yields were calculated for different feed ratios of glucose to ethanol, and decreases for higher ethanol fractions were correctly predicted for mutants with deletions of the malate synthase, the isocitrate lyase, or the phosphoenolpyruvate carboxykinase. The growth of the fructose- 1,6-bisphosphatase deletion mutant was anticipated less accurate, but the tendency was modeled correctly. © 2002 John Wiley & Sons, Inc. *Biotechnol Bioeng* **77**: 61–72, 2002.
Keywords: null mutants; *S. cerevisiae*; metabolic network model

INTRODUCTION

Advances in genetical engineering allow the specific alteration of the metabolic reactions and pathways, but due to the complexity of metabolic networks the outcome of these changes can be predicted intuitively in only few simple cases, mainly in applications concerning a specific production pathway of a secondary metabolite. Directed genetic alterations of the cells central metabolism require a more systematic approach (Bailey, 1991). Here, metabolic network analysis proved itself to be a valuable tool in predicting the behavior of the reaction network under various conditions (Christensen and Nielsen, 1999; Holms, 1996).

Metabolic network analysis examines the structure of a proposed metabolic network, thus identifying, e.g., parallel pathways, futile cycles, and conserved moieties. It further determines which reactions of a given network can be quantified for a chosen set of measured rates under standard conditions. Metabolic flux analysis is then applied to calculate the rates of these observable reactions. Depending on the structure of the network, both tools can be used to obtain the stoichiometrically conceivable yield of a desired product based solely on a set of biological feasible reactions (Vallino and Stephanopoulos, 1993) or its thermodynamically feasible yield by including energetic restrictions through the inclusion of the cofactor balances for NAD(P) and adenosine phosphates (van Gulik and Heijnen, 1995; van Gulik et al., 2001). The availability of sufficient data on a variety of steady state conditions allows the quantification of the cell's energetic parameters; the *P/O* ratio and the maintenance requirements as demonstrated by Gulik and Heijnen (1995) and Vanrolleghem et al. (1996).

The yeast *Saccharomyces cerevisiae* is able to metabolize glucose as well as ethanol. Despite the diauxic growth in batch culture, *S. cerevisiae* can use glucose and ethanol in mixed cultures simultaneously under carbon-limited conditions in continous chemostat cultures. Depending on the ratio of glucose and ethanol in the media, the activity of the glyoxylate cycle enzymes isocitrate lyase (ICL) and malate synthase (MLS) and the gluconeogenic enzymes phosphoenolpyruvate carboxykinase (PCK) and fructose-1,6-bisphosphatase (FBP) is needed at different values. It has been shown that the

Correspondence to: Hans Christian Lange, Kluyver Laboratory for Biotechnology, Delft University of Technology, Julianalaan 67, 2628 BC Delft, The Netherlands.

**Present address:* Aventis Pharma Deutschland GmbH, Frankfurt, Germany.

DOI 10.1002/bit.10123

onset of these enzymes is tightly regulated depending on the ratio of glucose and ethanol in the substrate (de Jong-Gubbels et al., 1995). By using single null mutants in the mentioned enzymes we could show the ratio of glucose and ethanol in the feed from which the activity of the single enzyme is needed for the complete utilization of both C-sources.

Vanrolleghem et al. (1996) as well as van Gulik and Heijnen (1995) successfully used the metabolic flux analysis to calculate the switching points of these key enzyme. In the presented work, we have now employed the metabolic flux analysis for the quantitative prediction of genetically modified *S. cerevisiae* based on knowledge about the unaltered strain. Biomass yields in carbon-limited chemostat fermentations were correctly forecasted over a range of different substrate mixtures based solely on network analysis and energetic parameters obtained from the corresponding wild-type strain for different null mutants, incapacitated in their glyoxylate cycle and their gluconeogenesis. Model predictions were verified with measured data obtained from chemostat cultures.

MATERIALS AND METHODS

Construction of Null Mutants

The haploid prototrophic wild-type strain *S. cerevisiae* CEN.PK 113-7D was used as reference for the derived knockout mutants. Haploid *S. cerevisiae* null mutants were constructed by replacing the genes coding for the enzymes malate synthase (*MLS1*), isocitrate lyase (*ICL1*), phosphoenolpyruvate carboxykinase (*PCK1*), and the fructose-1,6-bisphosphatase (*FBP1*) by the short flanking homology (SFH) method (Table I) (Wach et al., 1994). SFH deletion cassettes were made by PCR with primers homologous to both the kanamycin deletion cassette of plasmid pUG6 (Güldener et al., 1996) and the gene(s) of interest as described recently (Luttik et al., 1998). SFH-PCR products were first transformed in the diploid strain CEN.PK122 and subsequently the corresponding haploid deletion strains were obtaind by tetrad analysis. Mating type and the correct integration of the kanamycin deletion cassette were verified by PCR as described previously (Luttik et al., 1998). Standard techniques and media for genetic modification of *S. cerevisiae* were used (Ausubel et al., 1989). All strains designated as CEN are isogenic to the *S. cerevisiae* strain CEN.PK2 (Entian and Kötter, 1998; van Dijken et al., 2000).

Strain Cultivation and Analysis

The haploid wild-type strain *S. cerevisiae* CEN.PK113-7D was used as reference for the derived knockout mutants. The null mutants in the enzymes of the glyoxylate cycle enzymes malate synthase (mls) and isocitrate lyase (icl) and of the gluconeogenic enzymes phosphoenolpyruvate carboxykinase (pck) and fructose-1,6-bisphosphatase (fbp) were made with the kanamycin method (Güldener, et al., 1996 ID: 329) in the diploid *S. cerevisiae* wild-type strain CEN.PK122. The following obtained haploid mutant strains of *S. cerevisiae* were used for the experiments: CEN.PK233-lC(*mls1* Δ), CEN. PK229-4D(*icl1* Δ), CEN.PK46-1A(*pck1* Δ), CEN. PK255-1D (*fpb1* Δ).

The wild-type strain was grown aerobically in carbon-limited chemostat cultures using 2-L Applikon fermentors at different dilution rates between 0.025 and 0.2 h^{-1}, 30°C, and pH 5.0 on defined mineral media according to Verduyn et al. (1992) with either glucose, ethanol, or acetate as carbon source. The mutants were grown under the same conditions on glucose and ethanol in 1.5 L working volume at a dilution rate of $D = 0.1\ h^{-1}$ using Braun fermentors (B. Braun Biotech international, 2L). Dissolved oxygen tension remained always above 30%. The fermentors were inoculated with approximately 50 mL preculture, grown overnight on the same mineral medium and 10 g/L glucose as carbon source.

Experiments with varying glucose–ethanol feed were performed with a constant total carbon concentration of 250 m*M*. For the determination of the energetic parameters the feed concentration varied between 180 and 480 m*M* carbon for glucose, ethanol was fed at a concentration of 350 m*M*, acetate at 270 m*M*. Carbon balances were checked routinely and closed with a recovery of more than 95% for all cultures.

The fermentors were aerated with an airflow of approximately 1 vvm. Off-gas analysis for oxygen and carbon dioxide was performed only for the wild-type cells using a Servomex 1100A oxygen analyzer (Taylor Servomex Co., USA) and a Beckman 864 infrared detector (Rosemount Analytics, USA) respectively. Biomass concentrations were determined through filtration on nitro-cellulose filters (pore size 0.43 μm, Gelman Sciences, USA).

Biomass was harvested after reaching steady state. A culture was considered to be in steady state if the biomass concentration was constant for at least five dilution times and the biomass was devoid of cell cycle associated oscillations (Duboc et al., 1996). The cells were spun down and washed with demineralized water. The biomass was stored at −20°C until being freeze-dried for 48 h. The biomass was then further dried at 70°C for 48 h and stored at room temperature in a desiccator to obtain a reproducible reference state until further analysis.

Biomass was analyzed for its elemental and constituent content as described earlier. Biomass was assumed to contain protein, carbohydrates, lipids, RNA, DNA, water, and metals. Results of the elemental and the constituent analysis were matched using statistical reconciliation (Lange and Heijnen, 2001).

Enzyme Assays

For enzyme assays 5 mL of culture was harvested after reaching steady state by centrifugation. The biomass was stored at −20°C until being used. Crude extracts were prepared using glass beads for breaking the cells as described by Ciriacy (1973). The crude extract was then directly used for the enzyme assays.

Malate synthase and isocitrate lyase activity was determined according to Dixon and Kornberg (1959), phosphoenolpyruvate carboxykinase activity according to Hansen et al. (1976), and fructose bisphosphatase activity according to Gancedo and Gancedo (1971). Specific activities were computed as mU/mg protein, determined according to the microbiuret method (Zamenhoff, 1957) using bovine serum albumin as a standard.

Metabolic Network Analysis

Metabolic network analysis was performed with a network based on van Gulik and Heijnen (1995). Further reactions were included for the formation of the phosphatidates, precursors of phospholipids containing ethanolamine, choline, and serine. Different biomass-generating reactions were included to reflect the differences in measured biomass and protein composition in each steady state. Biomass, CO_2, and H_2O were assumed to be the only products of the metabolism (Appendix A).

Networks for glucose cultures were modeled using pyruvate carboxylase as anaplerotic reaction for the TCA cycle. NADPH was regenerated through the NADP dependent isocitrate dehydrogenase and the glucose-6-phosphate dehydrogenase with the pentose-phosphate (PP) pathway providing the required stoichiometric freedom for this cofactor. Networks for ethanol grown cultures included both NAD and NADP dependent aldehyde dehydrogenases. In this case the PP-pathway was restricted to provide pentose-phosphate precursors by removing the second transketolase, hereby removing a singularity introduced by the additional NAD-dependent aldehyde dehydrogenase. Gluconeogenesis follows the known route with PEP carboxylase and fructose bisphosphatase, replacing the pyruvate carboxylase and the phosphofructose kinase. The reactions of the glyoxylate cycle isocitrate lyase and malate synthase fulfill the anaplerotic requirements for the growth on C_2-components. The network for acetate is similar to the one used for the ethanol grown cultures with the sole exception of the use of the second transketolase to provide the freedom to generate the required NADPH in the PP-pathway.

In order to use the metabolic networks for predictions, the unknown energy requirements expressed in ATP of the assimilatory reactions and the amount of ATP spend on maintaining the current state of the cell have to be evaluated. These additional energetic requirements can be expressed with three energetic parameters: the P/O ratio, describing the efficiency of the oxidative phosphorylation, the growth related unknown ATP requirements for cell formation k, and the cell maintenance m_{ATP} of the organism (van Gulik and Heijnen, 1995). This energy demand can be solved using the ATP balance for each metabolic network:

$$q_o \cdot P/O - \mu \cdot k - m_{ATP} = q_{ATP}^{net}. \quad (1)$$

The specific rates q per C-mol biomass can be easily determined through metabolic flux analysis with q_o representing the moles of oxygen consumed for the reduction of NADH and FADH, and q_{ATP}^{net} being the amount of known ATP used in the specified anabolic and catabolic reactions. The q_{ATP}^{net} can be quantified by summarizing all reactions rates involving ATP except the regeneration through oxidative phosphorylation:

$$q_{ATP}^{net} = \sum v_{i,ATP} r_i. \quad (2)$$

Each biological steady state thus generates its distinct Eqs. (1) and (2). Using the appropriate metabolic network for Eq. (2), the energetic parameters P/O ratio, the growth related ATP requirements k, and the cell maintenance m_{ATP} can be obtained from data of minimal three distinct fermentations of the wild-type strain using linear regression techniques on Eq. (1). The accuracy of the estimated parameters is improved through the use of data from several chemostats with multiple substrates and a range of growth rates. The maintenance parameters m_{ATP} and k are be combined to k' for modeling purposes at a constant growth rate.

$$k' = k + \frac{m_{ATP}}{\mu}. \quad (3)$$

The flux analysis of the different null-mutants was done following the strategy outlined by van Gulik and Heijnen (1995) and Vanrolleghem and Heijnen (1998) who successfully applied it for the sequential enzyme expression during growth of *S. cerevisiae* on mixtures of glucose and ethanol (de Jong-Gubbels et al., 1995). As proposed in these papers, a set of different metabolic networks was used to model the complete range of the glucose–ethanol ratio in the feed.

RESULTS AND DISCUSSION

Biomass Composition

Metabolic flux analysis requires the description of the biomass not only in terms of its elements, but also in terms of its molecular composition. Therefore, the average composition for *S. cerevisiae* CEN.PK113-7D grown in carbon-limited chemostat at a dilution rate of $D = 0.1\ h^{-1}$ was analyzed for its elemental and molecular composition during growth on glucose, ethanol, and acetate as described previously (Lange and Heijnen,

Table I. Yeast strains used in this study.

Strain name	Relevant genotype[a]
CEN.PK113-7D	MATa URA3 HIS3 LEU2 TRP1 MAL2-8^c SUC2
CEN.PK122	MATa/MATα URA3/URA3 HIS3/HIS3 LEU2/LEU2 TRP1/TRP1 MAL2-8^c /MAL2-8^c SUC2/SUC2
CEN.PK229-4D	MATa URA3 HIS3 LEU2 TRP1 MAL2-8^c SUC2 icl1(41,1630)::loxP-Kan-loxP
CEN.PK233-1C	MATa URA3 HIS3 LEU2 TRP1 MAL2-8^c SUC2 mls1(41,1610)::loxP-Kan-loxP
CEN.PK255-1D	MATa URA3 HIS3 LEU2 TRP1 MAL2-8^c SUC2 fbp1(41,880)::loxP-Kan-loxP
CEN.PK487-1B	MATa URA3 HIS3 LEU2 TRP1 MAL2-8^c SUC2 cat8(44,299)::loxP-Kan-loxP
CEN.IS46-1A	MATa URA3 HIS3 LEU2 TRP1 MAL2-8^c SUC2 ppc1 (41,1610)::loxP-Kan-loxP

[a]The numbers in parentheses indicate the deleted nucleotides (ATG = 1) of the corresponding genes. All strains listed can be obtained from EUROSCARF (European *Saccharomyces cerevisiae* Archive for Functional Analysis) at http://www.rz.uni.frankfurt.de/FB/fb16/mikro/euroscarf/index.html.

Table II. Balanced elemental cell composition expressed as mass fractions f_i (in %).

	D (h^{-1})	f_C	f_H	f_N	f_O	f_P	f_S	f_M	Sum
Glucose	0.105	45.5	6.7	7.9	36.2	1.03	0.23	2.52	100.0
Ethanol	0.106	46.7	6.9	8.3	34.1	1.04	0.31	2.61	100.0
Acetate	0.106	46.5	6.9	8.9	33.8	1.05	0.32	2.48	100.0

2001). The elemental composition is presented in Table II. The molecular composition is described in terms of the mass fractions f of protein, carbohydrates, lipids, RNA, DNA, phosphate, sulfate, metals, and water. The different substrates led to significant changes in the biomass composition even while maintaining a constant growth rate. Glucose-grown cultures had a higher content of carbohydrates at $D = 0.1\ h^{-1}$, while biomass grown on the C_2-components ethanol and acetate was richer in lipids and proteins. Details of the reconciled biomass composition are given in Table III. Furthermore, the protein was analysed for its amino acid contents, an average composition (Table IV) was used for the calculations since no significant differences were found between the cultures. Biomass composition also shifted, e.g., to higher protein contents with increasing dilution rate as shown earlier (Lange and Heijnen, 2001), these changes were taken into account during the determination of the energetic parameters of the wild type. For the simulation of the mixed substrate growth, a linear interpolation of the values obtained for glucose and ethanol was used to reflecting the different biomass composition for pure glucose or ethanol growth, respectively. The ratio between both was linearly linked to the glucose–ethanol ratio in the feed.

Table IV. Average measured amino acid composition of protein (in mol %).

Ala	9.77	Met	1.14
Arg	3.86	Orn	0.24
Asx[a]	9.28	Phe	3.76
Cys	0.14	Pro	4.22
GIx[a]	15.48	Ser	5.33
GIy	8.89	Thr	5.57
His	1.93	Trp	0.65
Ile	5.89	Tyr	1.96
Leu	8.01	Val	7.33
Lys	6.57		

[a]Asx = Asp + Asn; GIx = GIm + GIn.

Determination of Energetic Parameters

The energetic parameters, P/O ratio, k_m and m_{ATP} the strain, were calculated based on results of 14 chemostats, 12 of which were grown on glucose under different growth rates and two with a growth rate of $D = 0.1\ h^{-1}$ grown on ethanol and acetate, respectively. The measurements underwent chi-square tests, the constraints being provided by the metabolic network. All data sets were consistent within a 95% confidence interval. Statistical reconciliation of the measurements were done according to van der Heijden et al. (1994) before the calculation of the energetic parameters. For $D = 0.1\ h^{-1}$ the average biomass yield was determined as 0.600, 0.623, and 0.382 $C\text{-}mol_{biomass}/C\text{-}mol_{substrate}$ for glucose, ethanol, and acetate, respectively. The yield on glucose increased from 0.483 to 0.624 $C\text{-}mol_{biomass}/C\text{-}mol_{substrate}$ with dilution rates increasing from 0.02 to 0.2 h^{-1} (Table V). Subsequently, the P/O ratio was determined for the metabolic network presented in Appendix A as 1.46, k_m as 655 $mmol_{ATP}/C\text{-}mol_{biomass}$, and m_{ATP} was evaluated to 56 $mmol_{ATP}/mol_{biomass}/h$. These values were then used for modeling of the deletion mutants on the range of mixed ethanol/glucose feeds.

However, the set of energetic parameters is dependant on the chosen network and can thus not be easily

Table III. Balanced elemental cell composition expressed as mass fractions f_i (in %).

Substrate	D (h^{-1})	$f_{protein}$	$f_{carbohyd.}$	f_{lipids}	f_{RNA}	f_{DNA}	f_{P_i}	f_{SO_4}	f_{water}	f_{metals}
Glucose	0.105	39.3	39.8	6.2	6.5	0.4	0.8	0.3	4.1	2.5
Ethanol	0.106	42.2	33.7	9.8	6.1	0.5	0.7	0.5	4.0	2.6
Acetate	0.106	45.1	30.9	8.7	6.8	0.5	0.6	0.5	4.4	2.5

Table V. Reconciled respiratory quotient (RQ) and yields (Y) on substrate and oxygen of *S. cerevisiae* CEN.PK113-7D.

Substrate	Dilution rate (h^{-1})	RQ (mol/mol)	Y_{xs} (C-mol/C-mol)	Y_{xo} (C-mol/mol-O_2)
Ethanol	0.106	0.45	0.623	0.74
Acetate	0.106	1.04	0.382	0.64
Glucose	0.022	1.06	0.483	0.99
	0.052	1.08	0.570	1.43
	0.087	1.07	0.586	1.51
	0.099	1.07	0.591	1.55
	0.104	1.08	0.620	1.77
	0.107	1.07	0.598	1.59
	0.107	1.07	0.613	1.70
	0.107	1.07	0.591	1.54
	0.108	1.06	0.571	1.41
	0.126	1.08	0.608	1.68
	0.158	1.09	0.620	1.78
	0.211	1.09	0.624	1.80

compared or transferred to other networks. Further improvements we introduced as the inclusion of ion transport, and a larger range of dilution rates had only minor effects on the energetic parameters. Furthermore, the biomass composition was measured for each steady state, the reconciled values Lange were used in the presented model. Calculations based on a single average biomass composition resulted in a 4% lower P/O value.

However, because the purpose of the used model is not to obtain a perfect description of the cell's energetics, but to provide a easy applicable tool, we tested the influence of the different parameters. Since a lower P/O ratio is compensated by the reduced requirements for maintenance, we found only small variations of less than 1.5% during the switching point determination when using a P/O value of 1.2.

Modeling of Growth of the Mutant Strains on Glucose–Ethanol mixtures

Five distinct networks were used to model the growth of the deletion mutants on glucose-ethanol mixtures, using a similar approach as suggested by van Gulik and Heijnenvan (1995). Each network spans a distinct range of glucose:ethanol ratios in the feed and is limited at each side by a certain ratio, the switching point, which requires a different set of enzymes to completely metabolise both substrates. With increasing ethanol content in the feed, the cell requires first simultaneously the two additional enzymes of the glyoxylate cycle, isocitrate lyase and malate synthase, followed by the gluconeogenic enzymes PEP carboxylase and fructose- 1,6-bisphosphatase. The three switching points were determined mathematically by solving an under-determined network for a "zero" flux for the particular reaction. For the modeling of the mutants, we assumed the same metabolism as for the wild type as long as the ratio of ethanol to glucose remained below the switching point of the missing enzyme. For higher ratios, the glucose will continue to be completely metabolised, but only a fraction of the provided ethanol will be taken up by the cell, thus effectively fixing the uptake ratio of glucose to ethanol to the value of the switching point. This will subsequently lead to a decrease of the apparent yield with higher ethanol fraction and to an accumulation of ethanol in the medium.

Mutants lacking either the malate synthase or the isocitrate lyase can use ethanol only to provide acetyl-CoA but not for anaplerosis. This has to be provided for by the glucose metabolism. Under the conditions used, i.e., a growth rate of 0.1 h^{-1} the metabolic network model predicts a maximum ethanol:glucose ratio of 48:52 on C-mol basis. Further ethanol will not be metabolized by the *mls1 Δ* or *icl1 Δ* mutants and will therefore remain in the broth. A strain lacking PEP carboxykinase can replenish the TCA cycle from ethanol but requires alternative substrates for glycolytic precursors. From this, the maximum uptake ratio of ethanol to total carbon for the pck1 *Δ* mutant was calculated as 59% (C mol ethanol/C mol carbon). The fructose bisphosphatase null mutant requires glucose for its C_6-precursors, the model predicts here a maximum ethanol fraction of 74%.

While the energetic parameters are very sensitive to the chosen metabolic network, the switching points remain almost the same, network variation rarely change the here presented points by more than 1%.

Verification of the Models by Chemostat Cultivation

The results of the metabolic flux model were compared with the actual measurements of the yield and the residual ethanol content in chemostat cultures. For the wild type the model anticipated an approximately constant biomass yield and no residual ethanol for the whole range of different ethanol to glucose ratios (Figs. 1A and 2A). For the different mutants, the model predicted a decrease in the biomass yield accompanied by the accumulation of ethanol for ratios exceeding the maximum ratio for the particular mutant. This was indeed observed in the chemostat experiments with the mutants. The *icl1 Δ* and the *mls1 Δ* mutants both exhibited the same linear decrease of the biomass concentration for ethanol fractions higher than 50% until complete disappearance for a 100% ethanol feed, agreeing well with the model prediction of 47% (Fig. 1B). The increase in the residual ethanol exhibited a slight lag compared to the predicted values. The lag might simply be attributed to evaporation. However, even at an ethanol content in the feed of 90% the predicted residual ethanol concentration (202 C mM, 4.7 g/L) is almost 20% higher than the measured 202 one (170 C mM, 3.9 g/L) (Fig. 2B).

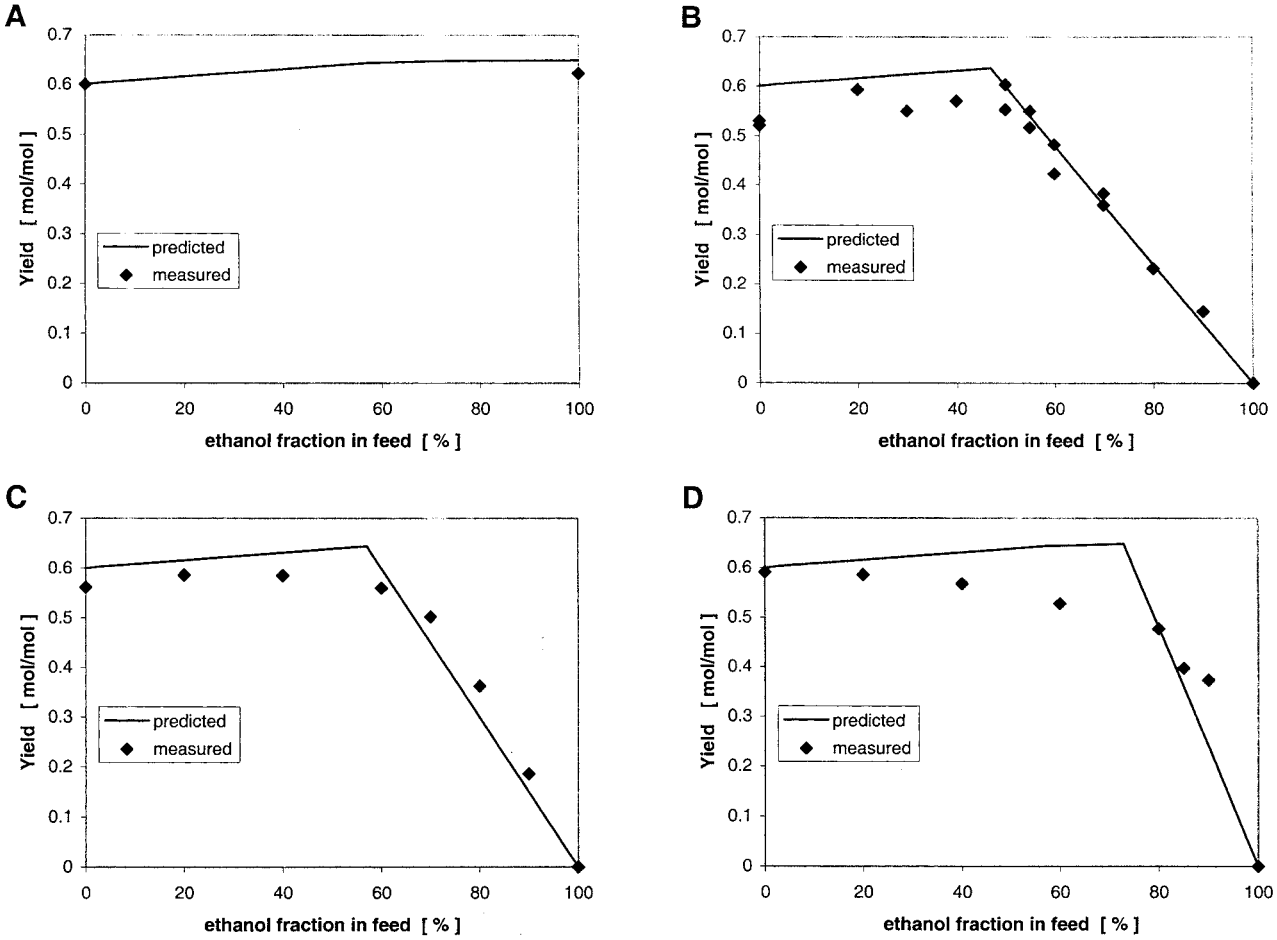

Figure 1. Predicted and measured biomass yields for *S. cerevisiae* grown in carbon-limited chemostat over the ratio of ethanol to glucose in the feed. (A) CEN.PKl 13-7D (wild type); (B) CEN.PK 233-1C (*mls1 Δ*) and CEN.PK 229-4D (*icl1 Δ*); (C) CEN.PK 46-1A (*pck1 Δ*); (D) CEN.PK 255-1D (*fbp1 Δ*).

For the PEP carboxykinase deletion mutant, the ethanol again starts to accumulate slightly later than predicted, but the increase follows the same slope as predicted. The measured biomass concentration starts to drop significantly below that of the wild type when the ethanol fraction in the feed exceeds 60%. The model predicts a sharp linear decrease at an ethanol fraction above 59%, thus model and measurements agree very well (Fig. 1C).

The fructose bisphosphatase deletion mutant shows a continued slow drop in biomass concentration already earlier than predicted by the model, which forecasted a sharp decline at an ethanol concentration above 74%. The measured residual ethanol concentration of 29.1 C m*M* (0.67 g/L) for the mutant at an ethanol concentration in the feed of 90% is significantly lower than the predicted value of 141 C m*M* (3.26 g/L), indicating a discrepancy between model prediction and real life behaviour of this mutant (Figs. 1D and 2D). Obviously, the cell's metabolism reacts in a more gradual fashion than envisioned by the model, possibly caused by changes in the biomass concentration.

In Fig. 3 the measured and predicted ethanol fractions of the consumed substrate have been plotted against the supplied ethanol fraction in the feed. All ethanol is consumed until the supplied ethanol fraction reaches the switching point. For higher ethanol fractions in the feed, the model predicts a constant consumed ethanol fraction. For the *fbp Δ* mutant the measurements and predictions do not compare very well. The measured data for the *pck Δ* and *icl Δ*/*mls Δ* mutants show some scatter. The average ethanol fraction of the consumed substrate is in both cases somewhat higher than predicted by the model.

Both the delayed onset of the ethanol accumulation as well as the slightly higher consumed ethanol fraction as observed in all cultures compared to the predicted value might be simply due to a shift in the biomass composition of the model. The yeast cell has the ability to adapt its composition according to its substrate source as

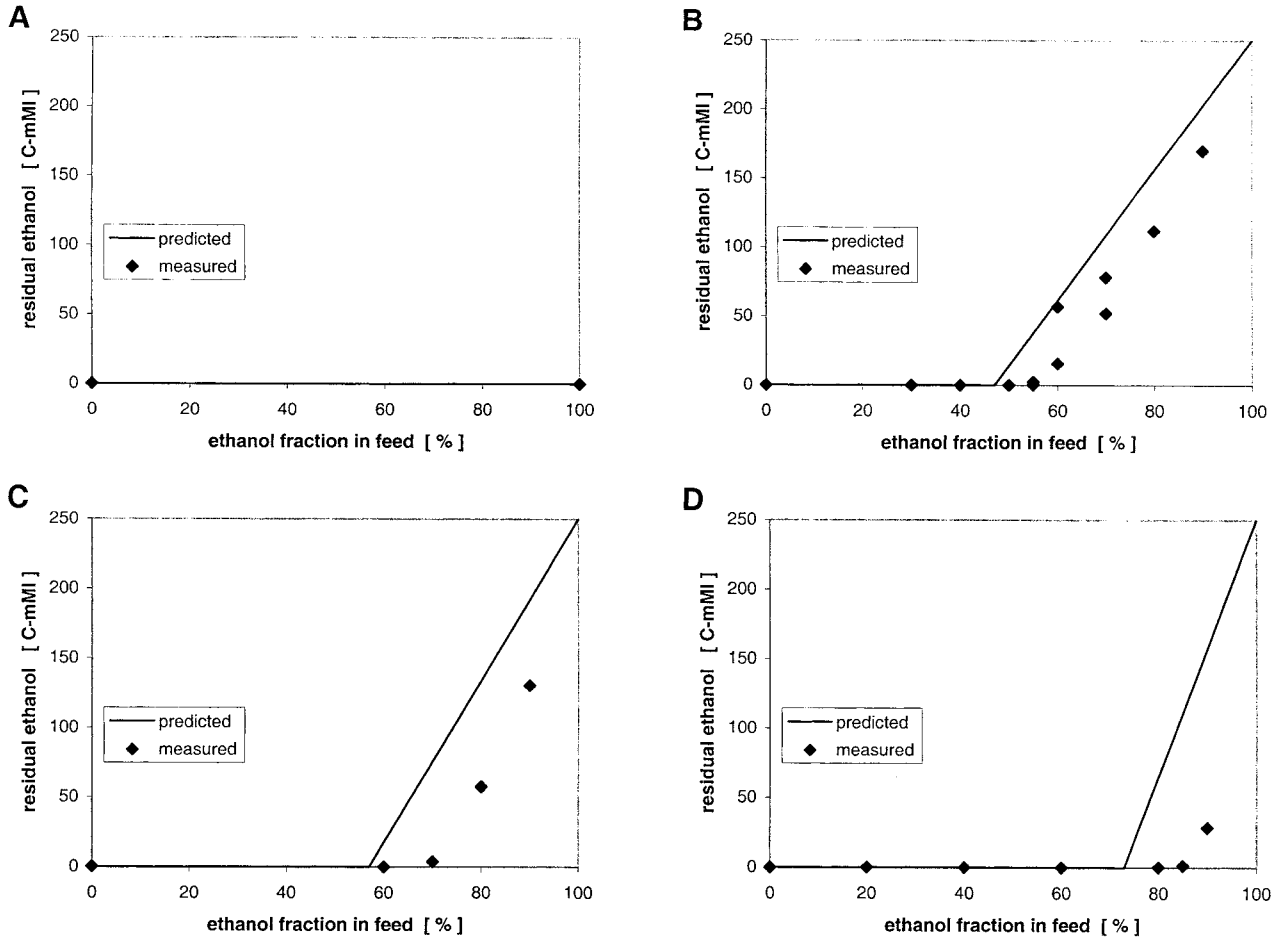

Figure 2. Predicted and measured residual ethanol for *S. cerevisiae* grown in carbon-limited chemostat over the ratio of ethanol to glucose in the feed. (A) CEN.PK113-7D (wild type); (B) CEN.PK 233-1C (*mls1 Δ*) and CEN.PK 229-4D (*icl1 Δ*); (C) CEN.PK 46-1A (*pck1 Δ*); (D) CEN.PK 255-1D(*fbp1 Δ*).

could be seen from the different biomass composition for glucose, ethanol, and acetate. It is therefore easily conceivable that a mutant unable to provide the required precursors for the anabolism of carbohydrates will instead have a relative higher abundance in other storage polymerse, e.g., lipids, and will thus be able to utilize a larger ethanol fraction.

CONCLUSIONS

A metabolic model based on four distinct networks was able to predict the quantitative growth of the *icl1 Δ*, the *mls1 Δ*, and the *pck1 Δ* mutants on mixtures of glucose and ethanol correctly. The model was based solely on the known pathways in yeast and the energetic parameters obtained in chemostat cultivations of the corresponding wild-type strain of *S. cerevisiae* CEN.PK113-7D. Quantitative agreement was less accurate for the *fbp1 Δ* mutant but was correct in its tendency. This demonstrates the capacity of metabolic flux analysis to correctly predict proposed genetical changes *in silico* before these are realized in vivo.

The experiments show the specific glucose–ethanol concentration from which the activity of the single enzyme is needed to metabolize both glucose and ethanol completely. These results also verify the statement from former publications (de Jong-Gubbels et al., 1995) that the activity of the four enzymes is needed one after the other beginning with isocitrate lyase and malate synthase over phosphoenolpyruvate carboxykinase to fructosebisphosphatase with rising ethanol content in mixed media.

Regulation of the enzymatic activity *in vivo* seems mainly to be caused by post-translational regulatory mechanisms such as allosteric effects and phosphorylation of the proteins since western blot experiments with the mentioned proteins (data not shown) reveals comparable protein concentrations of all four genes over the

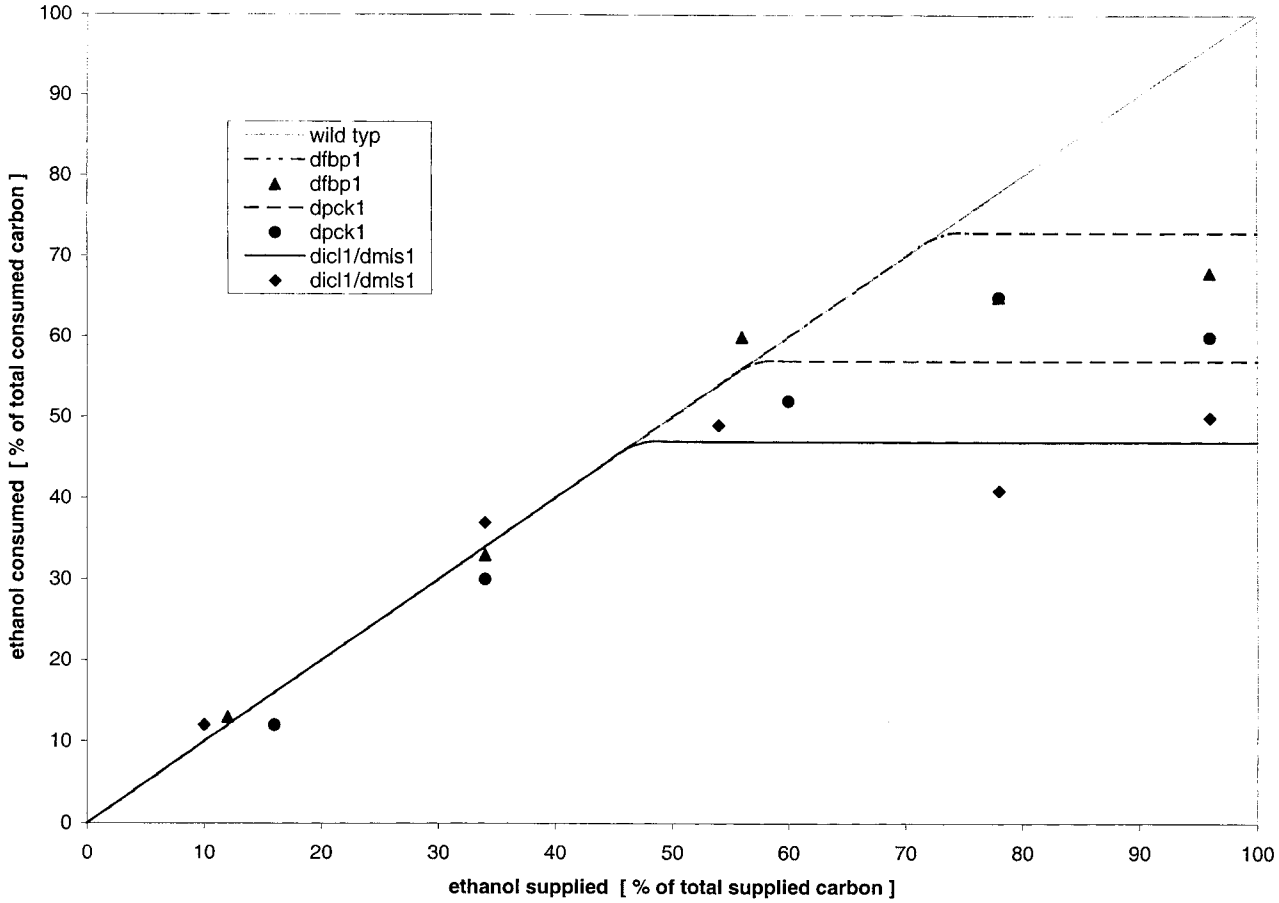

Figure 3. Consumed versus provided ethanol in the feed for *S. cerevisiae* in carbon-limited chemostat: (*) CEN.PK113-7D (wild type): (♦) CEN.PK 233-1C (*mls1 Δ*) and CEN.PK 229-4D (*icl1 Δ*): (●) CEN.PK 46-1A (*pck1 Δ*); (▲) CEN.PK 255-1D (*fbp1 Δ*).

experiments. Experiments with a deletion strain in the gene for Cat8p, an activator for the gluconeogenic genes (Hedges et al., 1995), shows behavior like the deletion strains for isocitrate lyase and malate synthase (data not shown). This result gives evidence that gene regulation is the same on the trancriptional level for all four genes. This conclusion is further supported by the fact, that the promotor sections of the four genes have the same regulatory elements (Caspary et al., 1997; Hedges et al., 1995; Proft et al., 1995; Schüller, 1994).

The results point to a tight post-translational regulation of the gluconeogenic enzymes which are expressed during growth on a glucose–ethanol mixture. The regulation of their *in vivo* activity is such as to prevent futile cycling. The control seem to rest solely with the available glucose and is independent of the external ethanol concentration.

NOMENCLATURE

D	dilution rate	(h^{-1})
f_i	mass fraction of component i in biomass	(%)
k'	combined maintenance coefficient	(mol ATP/C-mol biomass)
k_m	growth related maintenance	(mol ATP/C-mol biomass)
m_{ATP}	maintenance expressed in mol ATP	(mol ATP/C-mol biomass/h)
P/O	yield of ATP per oxygen atom	–
q_i	specific flow rate of component i	(mol/C-mol biomass/h)
r_i	specific reaction rate i	(mol/C-mol biomass/h)
μ	growth rate	(h^{-1})
v_{ij}	stoichiometric coefficient of component j in reaction i	–

Superscripts

net	related to the metabolic network
cat	related to catabolism
O	oxygen

APPENDIX A

List of Metabolic Reactions

Amino Acid Synthesis	
ALA N-trans	PYR + GLM $\rightleftharpoons$ OGL + ALA
ARG syn	ORN + CARP + ATP + ASP $\rightarrow$ AMP + ARG + FUM + 3 H + P_i + Ppi
ASN syn	H_2O + GLN + ATP + ASP $\rightarrow$ ADP + ASN + GLM + H + P_i
ASP N-trans	OXACT + GLM $\rightleftharpoons$ OGL + ASP
ASP kin	2 NADPH + 2 H + ATP + ASP $\rightarrow$ ADP + HSER + 2 NADP + P_i
CARP syn	2H_2O + GLN + CO_2 + 2 ATP $\rightarrow$ 2 ADP + CARP + GLM + 3 H + P_i
CYS syn	HCYS + SER + 2 H $\rightarrow$ CYS + NH_4 + OBU
GLM deh	NH_4 + NADPH + H + OGL $\rightarrow$ GLM + H_2O + NADP
GLM N-lig	NH_4 + GLM + ATP $\rightarrow$ ADP + GLN + H + P_i
GLY transf	THF + SER $\rightarrow$ GLY + H_2O + METHF
HCYS syn	H_2S + HSER + ACCoA $\rightarrow$ ACT + CoA + 2 H + HCYS
HIS syn	PRPP + 2 NAD + 3 H_2O + GLN + ATP $\rightarrow$ OGL + 6 H + HIS + 2 NADH + P_i + 2 PPi + AICAR
ILE N-trans	OBU + PYR + NADPH + H + GLM $\rightarrow$ OGL + CO_2 + H_2O + ILE + NADP
LEU N-trans	NAD + H_2O + GLM + OIV + ACCoA $\rightarrow$ OGL + CO_2 + CoA + H + LEU + NADH
LYS syn	2 NADPH + 2 NAD + H_2O + 2 GLM + ATP + ACCoA $\rightarrow$ OGL + AMP + CO_2 + CoA + H + LYS + 2 NADH + 2 NADP + PP_i
MET syn	HCYS + MYTHF + H $\rightarrow$ MET + THF
OIV syn	2 PYR + NADPH + 2H $\rightarrow$ OIV + CO_2 + H_2O + NADP
ORN syn	NADPH + H_2O + 2 GLM + ATP + ACCoA $\rightarrow$ ACT + ADP + OGL + CoA + NADP + P_i + ORN
PHE syn	H + GLM + CHO $\rightarrow$ OGL + CO_2 + H_2O + PHE
PRO deh	2 NADPH + 2 H + GLM + ATP $\rightarrow$ ADP + H_2O + 2 NADP + P_i + PRO
SER syn	3 PG + NAD + H_2O + GLM $\rightarrow$ OGL + H + NADH + P_i + SER
SHI path	2 PEP + NADPH + E_4P + ATP $\rightarrow$ ADP + CHO + NADP + 4 P_i
THR ald	THR $\rightarrow$ ACTAL + GLY
THR deh	THR + H $\rightarrow$ NH_4 + OBU
THR syn	HSER + H_2O + ATP $\rightarrow$ ADP + H + P_i + THR
TRP syn	SER + PRPP + GLN + CHO $\rightarrow$ CO_2 + GAP + GLM + H + H_2O + 2 P_i + PYR + TRP
TYR syn	NADP + GLM + CHO $\rightarrow$ OGL + CO_2 + NADPH + TYR
VAL N-trans	GLM + OIV $\rightleftharpoons$ OGL + VAL
Biomass Formation	
biom-A1	.01716 metal + .00385 DNA + .13456 LIPID + .00188 SO_4 + .05185 RNA + .29537 CARBHYD + .51428 PROT + .00163 P_i + .06329 H_2O $\rightarrow$ biom-Al_e
biom-E1	.01799 metal + .00375 DNA + . 15073 LIPID + .00186 SO_4 + .04611 RNA + .32015 CARBHYD + .47917 PROT + .00196 P_i + .05674 H_2O $\rightarrow$ biom-$E1_e$
biom-G1	.01812 metal + .00354 DNA + .12682 LIPID + .00114 SO_4 + .03005 RNA + .43765 CARBHYD + .40186 PROT + .00376 P_i + .05998 H_2O $\rightarrow$ biom-Gl_e
biom-G2	.01759 metal + .0035 DNA + .12144 LIPID + .00101 SO_4 + .03521 RNA + .39508 CARBHYD + .44469 PROT + .0032 P_i + .05661 H_2O $\rightarrow$ biom-$G2_e$
biom-G3	.01825 metal + .00353 DNA + .09754 LIPID + .00153 SO_4 + .04175 RNA + .39545 CARBHYD + .46165 PROT + .00295 P_i + .0545 H_2O $\rightarrow$ biom-$G3_e$
biom-G4	.01797 metal + .00362 DNA + .10086 LIPID + .00094 SO_4 + .04701 RNA + .39766 CARBHYD + .45077 PROT + .00245 P_i + .05611 H_2O $\rightarrow$ biom-$G4_e$
biom-G5	.01813 metal + .00404 DNA + .10711 LIPID + .00186 SO_4 + .04806 RNA + .38846 CARBHYD + .45225 PROT + .00227 P_i + .0595 H_2O $\rightarrow$ biom-$G5_e$
biom-G6	.01771 metal + .00352 DNA + .09751 LIPID + .00092 SO_4 + .05334 RNA + .3772 CARBHYD + .46835 PROT + .05874 H_2O $\rightarrow$ 00197 P_i + biom-$G6_e$
biom-G7	.01775 metal + .00355 DNA + .09786 LIPID + .00097 SO_4 + .04855 RNA + .4046 CARBHYD + .44537 PROT + .00243 P_i + .06556 H_2O $\rightarrow$ biom-$G7_e$
biom-G8	.01744 metal + .00291 DNA + .09669 LIPID + .00087 SO_4 + .0514 RNA + .37653 CARBHYD + .47239 PROT + .0021 P_i + .05991 H_2O $\rightarrow$ biom-$G8_e$
biom-G9	.01825 metal + .00376 DNA + .09084 LIPID + .00094 SO_4 + .05429 RNA + .38999 CARBHYD + .46104 PROT + .00198 P_i + .06367 H_2O $\rightarrow$ biom-$G9_e$
biom-G10	.0172 metal + .00351 DNA + .1092 LIPID + .00065 SO_4 + .04448 RNA + .377 CARBHYD + .46573 PROT + .00262 P_i + .06395 H_2O $\rightarrow$ biom-$G10_e$
biom-G11	.01764 metal + .00352 DNA + .11022 LIPID + .0015 SO_4 + .0461 RNA + .3492 CARBHYD + .49088 PROT + .00258 P_i + .06973 H_2O $\rightarrow$ biom-$G11_e$
biom-G12	.01748 metal + .00351 DNA + .10468 LIPID + .00179 SO_4 + .05141 RNA + .33304 CARBHYD + .50728 PROT + .00203 P_i + .0637 H_2O $\rightarrow$ biom-$G12_e$
C-1 Metabolism	
DHF red	DHF + NADPH + H $\rightarrow$ NADP + THF
METHF deh	NADPH + H + FTHF $\rightarrow$ H_2O + METHF + NADP
METHF red	NADPH + METHF + H $\rightarrow$ MYTHF + NADP

Catabolism	
SO_4 ass	SO_4 + 4 NADPH + 3 H + 2 ATP ADP + AMP + 2 H_2O + 4 NADP + P_i + PPi + H_2S
Gluconeogenesis	
F16P phos	F16P + H_2O F6P + P_i
ICIT lya	ICIT GLYO + SUC
MAL syn	H_2O + GLYO + ACCoA CoA + H + MAL
PEP ck	OXACT + ATP ADP + CO_2 + PEP
Glycolysis, Lower	
Enol	2PG H_2O + PEP
GAP deh	P_i + NAD + GAP H + NADH + 13PG
13PG kin	13PG + ADP ATP + 3PG
3PG mut	3PG 2PG
PYR kin	PEP + H + ADP ATP + PYR
Glycolysis, Upper	
F16P ald	F16P GAP + DHAP
G6P iso	G6P F6P
HX kin	GLUC + ATP ADP + G6P + H
PF kin	F6P + ATP ADP + H + F16P
TP iso	DHAP GAP
Lipid Synthesis	
ACCoA carb	H_2O + CO_2 + ATP + ACCoA ADP + 2H + P_i + MACoA
avFA form	4.4 PLLM-CoA + 1.4 PLM-CoA + 1.7 OLE-CoA + STE-CoA 8.5 avFA-CoA
avPL form	4 PHD-ETA + 11PHD-CHO + 3 PHD-SER 18 avPL
FAT form	AvFA-CoA + PHD + H_2O CoA + P_i + FAT
GOH_3P trans	2 avFA-CoA + GOH3P 2 CoA + PHD
GOH deh	DHAP + NADH + H NAD + GOH3P
MET Atrans	MET + 2 H_2O + ATP H + 3 P_i + SAM
PLM desat	PLM-CoA + O_2 + NADPH + H 2 H_2O + NADP + PLLM-CoA
PLM lig	PLM + H_2O + CoA + ATP AMP + H + 2 P_i + PLM-CoA
PLM syn	7MACoA + 14 NADPH + 20 H + ACCoA 7 CO_2 + 8 CoA + 6H_2O + 14 NADP + PLM
PHD-C trans	PHD + H_2O + CTP 2 P_i + CMP-DGOH
PHD-EA meth	3 SAM + PHD-ETA 3 H + PHD-CHO + 3 SAH
PHD-SER dec	PHD-SER CO_2 + PHD-ETA
PHD-SER syn	CMP-DGOH + SER CMP + PHD-SER
SAH hyd	SAH + H_2O H + HCYS + A
STE desat	STE-CoA + O_2 + NADPH + H 2 H_2O + NADP + OLE-CoA
STE ligase	STE + H_2O + CoA + ATP AMP + H + 2 P_i + STE-CoA
STE syn	8 MACoA + 16 NADPH + 23 H + ACCoA 8 CO_2 + 9 CoA + 7 H_2O + 16 NADP + STE
Macromolecule Synthesis	
avAA form	.02382 ORN + .73257 VAL + .19598 TYR + .06492 TRP + .55657 THR + .5328 SER + .42243 PRO + .37583 PHE + .11378 MET + .65699 LYS + .8008 LEU + .58939 ILE + .19258 HIS + .88918 GLY + 1.0214 GLM + .52618 GLN + .01387 CYS + .5199 ASP + .40849 ASN + .38557 ARG + .97695 ALA CARBHYD syn + H_2O + G6P + ATP ADP + H + 2 P_i + 6 CARBHYD
DNA poly	.2 GTP + .3 UTP + NADPH + .3 METHF + H + .2 CTP + .3 ATP H_2O + NADP + 9.8 DNA + PPi + .3 DHF
LIPID form	.45 avPL + .55 FAT 47.22 LIPID
PROT poly	2 H_2O + 3 ATP + avAA 2 ADP + AMP + 4 H + 2 P_i + 4.810233 PROT + Ppi
RNA syn	.2 GTP + .3 UTP + .2 CTP + .3 ATP 9.5 RNA + PPi
Nucleotide Synthesis	
A kin	H + AMP + ADP ATP + A
AMP kin	ATP + AMP 2 ADP
AMP syn	IMP + ATP + ASP ADP + AMP + FUM + 2 H + P_i
CTP syn	UTP + H_2O + GLN + ATP ADP + CTP + GLM + 2 H + P_i
CMP kin	CMP + ATP ADP + CDP
GMP syn	NAD + IMP + 2 H_2O + GLN + ATP AMP + GLM + GMP + 4 H + NADH + Ppi
GMP kin	GMP + ATP ADP + GDP
IMP syn	AICAR + FTHF H_2O + IMP + THF
GDP kin	GDP + ATP ADP + GTP
UDP kin	UDP + ATP ADP + UTP
CDP kin	CDP + ATP ADP + CTP
PRPP syn	RIBU5P + ATP AMP + H + PRPP
AICAR syn	PRPP + 2 H_2O + GLY + 2 GLN + FTHF + CO_2 + 4 ATP + ASP 4 ADP + FUM + 2 GLM + 8 H + 4 P_i + THF + PPi + AICAR
PPi ase	PPi + H_2O 2 P_i
UMP syn	PRPP + .5 O_2 + CARP + ASP CO_2 + 2 H_2O + P_i + UMP + Ppi
UMP kin	UMP + ATP ADP + UDP
Oxidative Phosphorylation	
FAD reg	.5 O_2 + FADH2 FAD + H_2O
NAD reg	.5 O_2 + NADH + H H_2O + NAD

OX_NADH	$1.46\ P_i + .5\ O_2 + NADH + 2.46\ H + 1.46\ ADP \rightarrow 1.46\ ATP + 2.46\ H_2O + NAD$
OX_$FADH_2$	$1.46\ P_i + .5\ O_2 + 1.46\ H + FADH_2 + 1.46\ ADP \rightarrow 1.46\ ATP + FAD + 2.46\ H_2O$
maintenance	$H_2O + ATP \rightarrow ADP + H + P_i$
Pentose Phosphate Pathway	
G6P deh	$2\ NADP + H_2O + G6P \rightarrow CO_2 + 2\ H + 2\ NADPH + RIBU5P$
RIBU iso	$RIBU5P \rightarrow RIB5P$
RIBUP epi	$RIBU5P \rightarrow XYL5P$
TA1	$SED7P + GAP \rightarrow E4P + F6P$
TK1	$XYL5P + RIB5P \rightarrow GAP + SED7P$
TK2	$XYL5P + E4P \rightarrow F6P + GAP$
Pyruvate Branchpoint	
ACTAL deh_NAD	$NAD + H_2O + ACTAL \rightarrow ACT + 2H + NADH$
ACTAL deh_NADP	$NADP + H_2O + ACTAL \rightarrow ACT + 2\ H + NADPH$
ACCoA syn	$H_2O + CoA + ATP + ACT \rightarrow ACCoA + AMP + H + 2\ P_i$
ETOH deh	$NADH + H + ACTAL \rightarrow ETOH + NAD$
LAC deh	$NAD + LAC \rightarrow H + NADH + PYR$
PYR carb	$PYR + H_2O + CO_2 + ATP \rightarrow ADP + 2\ H + P_i + OXACT$
PYR dec	$PYR + H \rightarrow ACTAL + CO_2$
PYR deh	$PYR + NAD + CoA \rightarrow ACCoA + CO_2 + NADH$
TCA Cycle	
ACON 1	$CIT \rightarrow H_2O + ACO$
ACON 2	$ACO + H_2O \rightarrow ICIT$
CIT syn	$OXACT + H_2O_e + ACCoA \rightarrow CIT + CoA + H$
FUM hy	$H_2O + FUM \rightarrow MAL$
ICIT deh_NAD	$NAD + ICIT \rightarrow OGL + CO_2 + NADH$
ICIT deh_NADP	$NADP + ICIT \rightarrow OGL + CO_2 + NADPH$
MAL deh	$NAD + MAL \rightarrow H + NADH + OXACT$
OGL deh	$NAD + CoA + OGL \rightarrow CO_2 + NADH + SUCCoA$
SUC deh	$SUC + FAD \rightarrow FADH_2 + FUM$
SUCCoA syn	$SUCCoA + P_i + ADP \rightarrow ATP + CoA + SUC$
Transport	
ACT trans	$2\ H_e + ACT_e \rightarrow ACT + 2\ H$
ATPase	$H_2O + ATP \rightarrow ADP + H_e + P_i$
ETOH trans	$ETOH \rightarrow ETOH_e$
CO_2 diff	$CO_2 \rightarrow CO_{2e}$
GLUC fdiff	$GLUC_e \rightarrow GLUC$
GOH trans	$H + GOH \rightarrow GOH_e + H_e$
H_2O diff	$H_2O \rightarrow H_2O_e$
LAC trans	$LAC_e + H_e \rightarrow H + LAC$
MET imp	$metal_e \rightarrow metal$
NH_4 trans	$NH_{4e} + H_e \rightarrow H + NH_4$
O_2 diff	$O_{2e} \rightarrow O_2$
P_i trans	$P_{ie} + 2\ H_e \rightarrow 2\ H + P_i$
PYR trans	$PYR_e\ 4\text{-}\ H_e \rightarrow H + PYR$
SO_4 trans	$SO_{4e} + 3\ H_e \rightarrow 3\ H + SO_4$

References

Ausubel F.M., Brent R, Kingston RE, et al. 1989. Short protocols in molecular biology New York: John Wiley & Sons Inc.

Bailey JE 1991. Toward a science of metabolic engineering. Science 252:1668–1675.

Caspary F, Hartig A, Schüller H-J. 1997. Constitutive and carbon source-responsive promoter elements are involved in the regulated expression of the *Saccharomyces cerevisiae* malate synthase gene *MLS1*. Mol Gen Genet 255:619–625.

Christensen B, Nielsen J. 1999. Metabolic network analysis: a powerful tool in metabolic engineering. Adv Biochem Eng/Biotechnol 66:209–231.

Ciriacy M. 1973. Genetics of alcohol dehydrogenase in *Saccharomyces cerevisiae*. I. Isolation and genetic analysis of mutants. Mutat Res 19:315–326.

de Jong-Gubbels P, Vanrolleghem PA, Heijnen JJ, van Dijken JP, Pronk JT. 1995. Regulation of carbon metabolism in chemostat cultures of *Saccharomyces cerevisiae* grown on mixtures of glucose and ethanol. Yeast 11:407–418.

Dixon GH, Kornberg HL. 1959. Assay methods for key enzymes of the glyoxylate cycle. Biochem J 72: 3.

Duboc P, Marison I, von Stockar U. 1996. Physiology of *Saccharomyces cerevisiae* during cell cycle oscillations. J Biotechnol 51: 57–72

Entian K-D, Kötter P. 1998. Yeast mutant and plasmid collections. In: Brown AJP, Tuite MF, editors. Methods in microbiology, Vol. 26. London: Academic Press.

Gancedo JM, Gancedo C. 1971. Fructose-1,6-diphosphatase, phosphofructokinase, and glucose-6-phosphate dehydrogenase from fermenting and non-fermenting yeast. Biotechnol Bioeng 76:132–138.

Güldener U, Heck S, Fielder T, Beinhauer J, Hegemann JH. 1996. A new efficient gene disruption cassette for repeated use in budding yeast. Nucleic Acids Res 24:2519–2524.

Hansen RJ, Hinze H, Holzer H. 1976. Assay of phosphoenolpyruvate carboxykinase in crude yeast extracts. Anal Biochem 74:576–584.

Hedges D, Proft M, Entian K-D. 1995. *CAT8*, a new zinc cluster-encoding gene necessary for depression of gluconeogenic enzymes in the yeast *Saccharomyces cerevisiae*. Mol Cell Biol. 15:1915–1922.

Holms H. 1996. Flux analysis and control of the central metabolic pathway in *Escherichia coli*. FEMS Microbiol Rev 19:85–116.

Lange HC, Heijnen JJ. 2001. Statistical reconciliation of the elemental and polymeric biomass composition of *Saccharomyces cerevisiae* Biotechnol Bioeng 75:334–344.

Luttik MAH, Overkamp KM, Kötter P, de Vries S, van Dijken JP, Pronk JT. 1998. The *Saccharomyces cerevisiae* NDE1 and NDE2 genes encode seperate mitochondrial NADH dehydrogenases catalyzing the oxidation of cytosolic NADH. J Biol chem 273:24529–24534.

Proft M, Grzesitza D, Entian K-D. 1995. Identification and characterization of regulatory elements in the phosphoenolpyruvate carboxykinase gene *PCK1*. of *Saccharomyces cerevisiae*. Mol Gen Genet 246:367–373.

Rizzi M, Theobald U, Querfurth E, Rohrhirsch T, Baltes M, Reuss M. 1996. In-vivo investigation of glucose transport in *Saccharomyces cerevisiae*, Biotechnol Bioeng 49:316–327.

Schüller H-J. 1994. A carbon source-responsive promoter element necessary for activation of the isocitrate lyase gene *ICL1* is common to genes of the gluconeogenic pathway in the yeast *Saccharomyces cerevisiae*. Mol Cell Biol 6:3613–3622.

Vallino JJ, Stephanopoulos G. 1993. Metabolic flux distributions in *Corynebacterium glutaminum* during growth and lysine overproduction. Biotechnol Bioeng 41:633–646.

van der Heijden RTJM, Heijnen JJ, Hellinga C, Romein B, Luyben KChAM. 1994. Linear constraint relations in biochemical reaction systems. I. Classification of the calculability and the balanceability of conversion rates. Biotechnol Bioeng 43:3–10.

van Dijken JP, Bambilla L, Bauer J, et al. 2000. An interlaboratory comparison of physiological and genetic properties of four *Saccharomyces cerevisiae* strains. Enzyme Microbiol Technol 26:706–714.

van Gulik WM, Antoniewicz MR, de Laat WT, Vinke JL, Heijnen JJ. 2001. Energetics of growth and penicillin production in a high-producing strain of *Penicillium chrysogenum*. Biotechnol Bioeng 72:185–193.

van Gulik WM, Heijnen JJ. 1995. A metabolic network stoichometry analysis of microbial growth and product formation. Biotechnol Bioeng 48:681–698.

Vanrolleghem PA, de Jong-Gubbels P, van Gulik WM, Pronk JT, van Dijken JP, Heijnen JJ 1996. Validation of a metabolic network for *Saccharomyces cerevisiae* using mixed substrate studies. Biotechnol Prog 12:434–448.

Vanrolleghem PA, Heijnen JJ. 1998. A structured approach for selection among candidate metabolic network models and estimation of unknown stoichiometric coefficients. Biotechnol Bioeng 58: 133–138.

Verduyn C, Postma E, Scheffers WA, van Dijken JP. 1991. A theoretical evaluation of growth yields of yeasts. Antonie van Leeuwnhoek 59:49–63.

Verduyn C, Postma E, Scheffers WA, van Dijken JP. 1992. Effect of benzoic acid on metabolic fluxes in yeasts: a continuous culture study on the regulation of respiration and alcoholic fermentation. Yeast 8:501–517.

Wach A, Brachat A, Pöhlmann R, Philippsen P. 1994. New heterologous modules for classical or PCR-based gene disruptions in *Sacharomyces cerevisiae*. Yeast 10:1793–1994.

Zamenhoff S. 1957. Preparation and assay of deoxyribonucleic acids from animal tissue. Methods enzymol 3:696–704.